GEOPHYSICS, VOL. 71, NO. 2 (MARCH-APRIL 2006); P. A7–A11, 4 FIGS.
10.1190/1.2187711

DOI:10.1190/1.2187711

A novel application of time-reversed acoustics: Salt-dome flank imaging using walkaway VSP surveys

Mark E. Willis[1], Rongrong Lu[1], Xander Campman[1], M. Nafi Toksöz[1], Yang Zhang[1], and Maarten V. de Hoop[2]

ABSTRACT

In this paper we present initial results of applying Time-Reversed Acoustics (TRA) technology to salt-dome flank, seismic imaging. We created a set of synthetic traces representing a multilevel, walkaway VSP for a model composed of a simplified Gulf of Mexico vertical-velocity gradient and an embedded salt dome. We first applied the concepts of TRA to the synthetic traces to create a set of redatummed traces without having to perform velocity analysis, moveout corrections, or complicated processing. Each redatummed trace approximates the output of a zero-offset, downhole source and receiver pair. To produce the final salt-dome flank image, we then applied conventional, poststack, depth migration to the zero-offset section. Our results show a very good image of the salt when compared to an image derived using data from a downhole, zero-offset source and receiver pairs. The simplicity of our TRA implementation provides a virtually automated method to estimate a zero-offset, seismic section as if it had been collected from the reference frame of the borehole containing the VSP survey.

INTRODUCTION

Time-Reversed Acoustics (TRA) exploits the time symmetry of the wave-equation symmetry in a number of nonseismic technologies, such as sonar, medical, and nondestructive testing. TRA is also referred to as Time-Reversal Mirrors (TRM) and Time-Reversal Cavities (TRC) (Fink, 1992; Derode et al., 2000; Fink and Cassereau, 2000; Fink and de Rosny, 2002; Jonsson et al., 2004). These physical experiments measure a recorded wavefield from a sound source, time reverse the recorded pressures or displacements, and reinject the time-reversed, recorded signals into the medium at the recording locations. This process efficiently back-propagates or retrofocuses the signal to the original source location.

In seismic literature *acoustic daylight imaging* and *seismic interferometry* are terms used to describe this also. To extract the earth Green's function between receivers, seismologists use natural and complex seismic sources, such as, ambient noise, microearthquakes, and drilling sounds (de Hoop and de Hoop, 2000; Schuster et al., 2003; Malcolm et al., 2004; Wapenaar, 2004; van Manen et al., 2005). Based on these principles, the Virtual Source (VS) method (Calvert et al., 2004; Bakulin and Calvert, 2004) overcomes the effects of shallow-overburden complications. Using seismic interferometry, the VS method essentially redatums surface seismic sources to a set of receivers placed in a nearly horizontal borehole directly below. This process creates prestack data as if each borehole receiver were both a source and a receiver, thus potentially improving the reservoir image quality at depth.

In this paper we image a salt-dome flank from a walkaway VSP. So we change from the VS geometry of a nearly horizontal well to a vertical well. Similarly to the VS method, we can redatum the surface seismic sources to create prestack traces collected from the borehole perspective. As with the VS method, we gain the advantage of not needing to address overburden corrections for statics, multiples, or velocity. If we limit our interest to background-velocity fields which allow for turning rays, e.g., the Gulf of Mexico, we further simplify the process by only generating the zero-offset section traces: the degenerative form of seismic interferometry. Then we performed a poststack depth migration of the zero-offset section. This methodology requires very little preprocessing which is especially important for field quality control, near real-time processing, and quick turnaround projects. By not creating the prestack traces, we lose the ability to use nonnormal incident (from the perspective of the borehole) reflection energy

Manuscript received by the Editor July 22, 2005; revised manuscript received October 4, 2005; published online March 1, 2006.
[1]Massachussets Institute of Technology, Earth Resources Laboratory, Cambridge, Massachusetts 02139. E-mail: mewillis@mit.edu; lurr@mit.edu; xander@erl.mit.edu; toksoz@mit.edu.
[2]Formerly Colorado School of Mines, Center for Wave Phenomena, Golden, Colorado 80401-1887; presently Purdue University, Center for Computational and Applied Mathematics, West Lafayette, Indiana 47907. E-mail: mdehoop@math.purdue.edu.

DOI:10.1190/1.2187711

but gain the advantage of omitting the conventional stacking process. At a later time the nonzero-offset traces may be generated using full seismic interferometric methods (Calvert et al., 2004), and fully processed to improve the image quality. In areas without turning-ray energy, the zero-offset traces will likely be of very little value, because most of the energy reflected off the salt-dome flank will escape the surface-recording aperture.

PRINCIPLES OF TIME-REVERSAL ACOUSTICS

In this paper we compare our methodology to the physical experiment of collapsing the recorded energy back to only the source location. This is the zero offset or degenerative case of seismic interferometry. The literature cites many different approaches to derive the theories and technologies related to the nonzero-offset case of TRA (Cassereau and Fink, 1992; Draeger et al., 1997; Derode et al., 2003; Snieder, 2004; Wapenaar, 2004; Schuster et al., 2004; Wapenaar and Fokkema, 2005). However, we can simplify all of them down to two basic principles: 1) the time symmetry of the wave equation and 2) the estimation and use of the Green's function for a collocated source and receiver in a medium. To these we will add our own principle about the value of the back-propagated signal.

Principle 1 — The wave equation can be run forward and backward

The first basic TRA principle is that the acoustic- and elastic-wave equations are symmetric with respect to time. Suppose we observe the outward-expanding wavefield from a point source inside a medium. Further, suppose we capture the wavefield at all points and for all time on an enclosed contour or surface surrounding the source but at some distance away. Then if we time reverse the recorded signals and reinject them into the medium from the recording locations, all of the energy will propagate completely back to the original source point. (This demonstrates the Kirchhoff-Helmholtz theorem that states: The boundary measurements can be used as Huygens' sources to extrapolate the wavefield to any point inside the medium.) The principle that a signal will propagate between its original source position and an arbitrary surrounding contour according to the wave equation applies equally well to both numerical modeling and physical experiments.

Principle 2 — A zero-offset trace at the source location can be estimated from autocorrelations of the recorded traces

The second basic TRA principle involves estimating the Green's function $g(t)$ and using it to back-propagate a recorded signal $r_j(t)$ at a receiver location x_j to the original source location x_s.

Suppose we place a delta-source function $\delta(t)$ at location x_s and record the resulting motion of the medium at a receiver $r_j(t)$ elsewhere in the medium. Because we used a delta-function source, the recorded motion is a direct measurement of the medium Green's function $g_j(t)$ between the source location and the receiver location as given by

$$r_j(t) = \delta(t) * g_j(t) = g_j(t). \tag{1}$$

Further, source-receiver reciprocity tells us that the source and receiver may be interchanged with no change in the Green's function. Unfortunately, we can never actually inject a delta-source function, so we must use a band-limited, causal-source function $s(t)$. So instead of measuring the Green's function $g_j(t)$ directly, we obtain recorded signal $r_j(t)$ using the equation

$$r_j(t) = s(t) * g_j(t). \tag{2}$$

To back-propagate the wavefield, first we time reverse our recorded waveform $r_j(t)$ and then propagate it from the receiver toward the source. Because, according to reciprocity, the Green's function from the receiver to the source is the same $g_j(t)$, the desired signal $\hat{s}_j(t)$ recorded at the original source location x_s is given by

$$\hat{s}_j(t) = r_j(-t) * g_j(t) = s(-t) * g_j(-t) * g_j(t). \tag{3}$$

Using the TRA operation, the signal $\hat{s}_j(t)$ at the source location is simply the back-propagated, recorded signal $r_j(t)$. Note that $g(-t) * g(t)$ is an estimate of the Green's function of the medium for the collocated source and receiver, but it does not include the contributions from all receivers on the full contour. Using the Kirchhoff-Helmholtz theorem in a manner following Derode et al., (2003), we now obtain a better estimate of the back-propagated trace using all recorded traces on the contour enclosing the source. We convolve each time-reversed trace with its Green's function and then sum them to obtain a better estimate of the signal that would have been recorded at the source location using

$$\begin{aligned}\hat{s}(t) &= \sum_j \hat{s}_j(t) = \sum_j s(-t) * g_j(-t) * g_j(t) \\ &= s(-t) * \sum_j g_j(-t) * g_j(t).\end{aligned} \tag{4}$$

The correct estimation of the Green's function $g_j(t)$ is crucial to this back propagation process. However, instead of using the exact Green's function, which we don't know, we use the recorded signal itself as an empirical Green's function. So we convolve the recorded signal $r_j(t)$ with its time-reversed version $r_j(-t)$ giving

$$\tilde{s}_j(t) = r_j(-t) * r_j(t) = [s(t) * s(-t)] * [g_j(t) * g_j(-t)]. \tag{5}$$

We accomplished the back propagation of the energy from this receiver to the source location with only one complication (compare equations 3 and 5): We end up with the autocorrelation of the original-source function given by $s(-t)^* s(t)$. (Note *autocorrelation* is defined as the convolution of a function with a time-reversed copy of itself.) Thus it is easy to back-propagate any trace from its recorded location to the original-source location by only performing its autocorrelation. Afterwards, we can use deconvolution to correct the source wavelet shape to compensate for the loss of the wavelet-phase term.

As we did for equation 4, we must now perform the estimate for all recorded traces by summing the autocorrelations for all individual receivers of a common source. If N is the number of receivers, our estimate of the back-propagated signal at the

source location is given by

$$\tilde{s}(t) = \sum_{j=1}^{N} r_j(-t) * r_j(t)$$
$$= s(t) * s(-t) * \sum_{j=1}^{N} g_j(-t) * g_j(t). \qquad (6)$$

Just as in the well-developed seismic-migration literature, the accuracy of this process is determined by how much desired seismic energy is captured by the enclosed-contour portion around the source and recorded by the seismic field acquisition (Cassereau and Fink, 1992; Derode et al., 2003). In addition, since we have not derived the exact handling of the boundary conditions for an arbitrary enclosed contour, our image may only be kinematically correct. However, for a marine, walkaway VSP acquisition in a $v(z)$ medium, this process may be useful in quick-turnaround applications where true amplitudes are not critical (as shown below).

Principle 3 — The estimated zero-offset trace at the source contains the normal-incident reflectivity

In the general nonseismic TRA literature, the medium is assumed to contain a random distribution of scatterers. Therefore the value of the back-propagated signal is described as only containing the source wavelet at zero time. Claims are made that at all other times the energy cancels out. However, general seismic literature shows us that the zero-offset trace contains normal-incident reflectivity. While the energy at zero time is related to the source wavelet, our back-propagated trace contains the recorded reflections that would have been observed at the source location from all scatterers or reflectors in the medium. The great value of this principle is that by simply summing the autocorrelations of appropriate sets of traces, we obtain an estimate of the zero-offset trace without the complexities of velocity analysis or moveout corrections.

VSP VELOCITY MODEL AND SYNTHETIC SEISMIC TRACES

Using simplified velocities from the SEG/EAGE 3D salt model (Aminzadeh et al., 1997), we built a 2D salt-dome velocity model (Figure 1). The model dimensions are 10 km in width (x direction) by 5 km in depth (z direction) with absorbing boundaries on all sides. The velocity model is sampled at 5-meter grid spacing. The source is a 30 Hz, center–frequency, Ricker wavelet. The background velocity is described by a compaction gradient given by $V(z) = V_0 + z \cdot K$ where V_0 is the initial velocity of the top layer and K is the velocity gradient. The salt dome has a P-wave velocity of 4480 m/s. Just as in the SEG/EAGE model, we introduce horizontal reflectors into the background velocity field using five, 15%-higher velocity spikes.

Our preferred processing geometry is a reverse VSP (RVSP) having sources at multiple borehole depths and receivers at the surface. In contrast, the preferred field-acquisition geometry is usually surface sources and downhole receivers. In either case, reciprocity may be invoked to sort the traces into an equivalent-RVSP geometry. We directly generated an RVSP with the well located at x = 7.5 km and with 100 sources ranging in depth from 1.6 km to 4.1 km, spaced 25 m apart. The 400 receivers were distributed 25 m below the surface, spaced 25 m apart. Figure 2 shows the horizontal component v_x for one common-shot reverse VSP, or equivalently, one common-receiver depth level for a conventional VSP. We used an elastic, finite-difference, modeling algorithm and set the shear-wave velocities to be as small as possible, making this effectively an acoustic model. Because of boundary absorbtion no free surface reflections were generated.

THE ZERO-OFFSET, DOWNHOLE-ACQUISITION CONCEPT

Suppose it were possible to construct a downhole VSP tool with a coincident seismic source and receiver. If this tool were feasible, we could collect single-fold, zero-offset, seismic data that could investigate the subsurface from the bore-

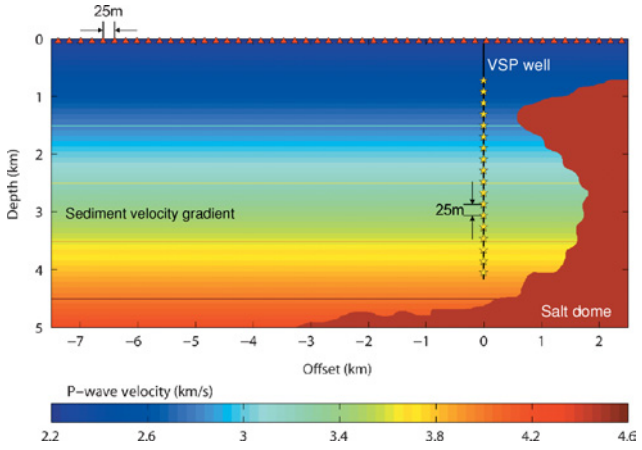

Figure 1. Salt-dome velocity model and P-wave velocity profile. The triangles indicate receiver, and the stars indicate source locations.

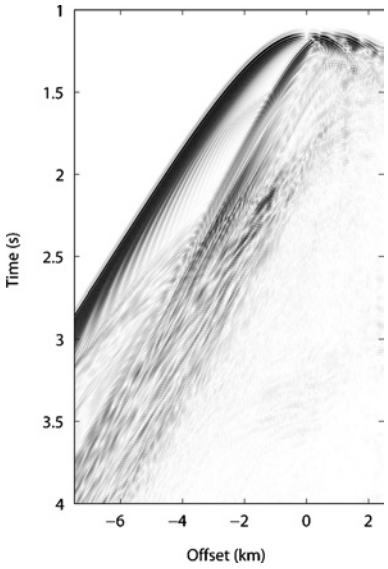

Figure 2. The horizontal component of motion v_x for one common-shot reverse VSP, or equivalently, one common-receiver depth level for a conventional VSP.

DOI:10.1190/1.2187711

hole vantage point. If the VSP tool were located in a well near a salt-dome flank, each recorded trace would contain important information about the reflections off the salt-dome flanks. In fact, each trace would contain the Green's function $\sum_j g_j(-t) * g_j(t)$ of the collocated source and receiver, albeit filtered by the source wavelet. Granted, this process will record the source wavelet at zero time, but the trace also will show reflected energy that can be used to create an image of the salt dome at later times. While this may seem obvious to traditional seismic-modeling and migration experts, nonseismic TRA studies may have obscured this point.

PROCESSING METHODOLOGY

The basic tasks we need to perform are to 1) back-propagate the recorded VSP data to each borehole sensor position and 2) migrate the traces to their proper subsurface position. A more detailed description of these steps is as follows:

1) Sort the VSP data into the proper gathers. If the data were recorded as a conventional walkaway VSP, then resort the data into the equivalent of an RVSP data set. To do this, sort the traces into VSP common-geophone gathers and call these "RVSP common-shot gathers." If the data were collected as RVSP data, then the data are naturally in RVSP common-shot gathers.
2) To enhance the direct and reflected events, preprocess the VSP data to eliminate borehole-guided waves. Preprocessing is very important for actual VSP data. However, our model study used an acoustic medium, so it is beyond the scope of this paper to address these specific steps.
3) For each common-shot gather, sum the autocorrelations of each trace. This operation produces the downhole, zero-offset, stacked trace along the well bore for each VSP instrument depth.
4) To each stacked trace, apply a wavelet-shaping operator to take the zero-phase, autocorrelated source wavelet back to a minimum-phase wavelet. We did not apply this step in our example, but it normally would be performed as a part of routine processing.
5) To produce an image of the salt-dome flank, perform conventional poststack reverse-time depth migration from the borehole reference frame on the zero-offset, stacked traces. This is the first time we use a velocity field, i.e., the background or regional-vertical gradient without salt and spikes in the model.

RESULTS

The top panel in Figure 3 shows the combined energy from vertical and horizontal components of the back-propagated, zero-offset VSP traces. For reference, each one of the traces in these panels comes from the sum of the autocorrelations of the traces in an RVSP common-shot record, e.g., as shown in Figure 2. To check the accuracy of our methodology, the bottom panel in Figure 3 shows the corresponding combined energy in the actual, zero-offset traces created during modeling. These zero-offset traces are comparable to the best results we could have achieved with our processing methodology if we had buried receivers on a contour that completely enclosed the source, instead of placing them on the surface. Most prominent on the actual zero-offset traces are the large-amplitude, spatially-coherent diffraction events with apexes at times between about 0.5 and 1.6 seconds. These events are reflections from the protruding rugosities of the salt-dome flank. Comparing these diffractions to the corresponding events on the back-propagated traces, we see that our method somewhat attenuated these events, especially at RVSP common-source depths above 2 km and below 3.5 km. On the back-propagated traces, we also see upgoing, linear events while the actual traces show events both upgoing and downgoing. These are the reflections from the background-model horizontal events. The acquisition geometry precluded recording the downgoing energy, so it is missing from the final results. The back-propagated traces show significant noise, especially at times before 0.5 seconds. This noise is because of the limited aperture of surface receivers. In fact, were it not for turning-ray energy created by the $v(z)$ medium or a similar velocity field, we most likely would not have captured enough energy to image the salt-dome flank. This comparison shows that our method captured the essence of the desired signal.

The middle panel in Figure 4 shows the result of performing a conventional, poststack reverse-time depth migration on our back-propagated traces shown in Figure 3. We combined the two vertical and horizontal components into an equivalent-pressure response. The left panel shows the result of depth migrating the actual zero-offset traces while the right panel shows the correct position of the salt-dome flank in the velocity model. Our back-propagated image does a very good job of recreating the salt-dome flank outline. However, it does not do a good job of recreating the horizontal layers image seen at depths of 2.5, 3.5, and 4.5 km on the migration of the actual zero-offset traces. This energy was recreated only weakly in the back-propagated wavefield but could not compete in the image with the early section noise. However, the turning-ray energy reflected off the salt-dome flank was faithfully back-

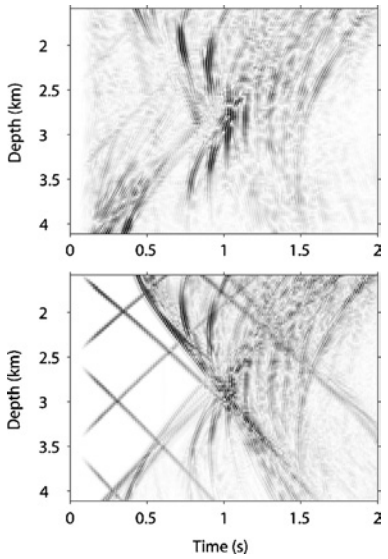

Figure 3. Comparison between the back-propagated VSP traces (top) and the actual signals recorded by the receivers located at the source positions (bottom). Both panels show the energy of the combined vertical and horizontal components.

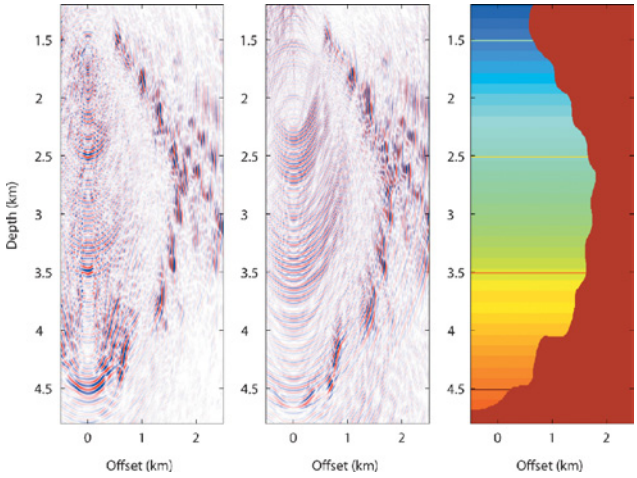

Figure 4. Comparison between the final migrated images from the back-propagated VSP traces (middle) and the actual signals recorded by the receivers located at the source positions (left). The right panel shows the actual-velocity model.

propagated to the source location and imaged in its proper location.

CONCLUSIONS

We extended the concepts found in nonseismic, time-reverse acoustics (TRA) literature to an exploration-seismic application of a multilevel, walkaway VSP. The TRA concepts allow us to back-propagate the recorded VSP data to a zero-offset downhole-reflection seismic experiment. Contrary to most of the nonseismic TRA literature, we assert that the zero-offset trace contains important imaging information that is normally discarded or ignored by other studies. The back propagation is accomplished using simple autocorrelations without the use of velocity analysis, prestack migration, or normal moveout corrections. The simplicity of this process makes it possible to perform concurrently with field acquisition to create fully automated, kinematically correct images. The results we obtained on acoustic-model data suggest that the method may be very effective for processing VSPs collected in the Gulf of Mexico where turning rays provide reflections from the undersides and salt-dome flanks. Future work to extract true-amplitude images needs to address the issues associated with the exact handling of boundaries and surface-related multiples.

Images created by performing conventional reverse-time, depth migration of the back-propagated, zero-offset data show clear definition of salt-dome flanks. These images are in good agreement with those created from actual zero-offset traces and provide strong encouragement about the value of this methodology for locating the lateral extent and dimensions of salt-dome flanks, especially in the Gulf of Mexico.

ACKNOWLEDGMENTS

We would like to thank Rama Rao and Daniel Burns for numerous helpful discussions on this topic as well as the anonymous reviewers who made excellent suggestions. This work was funded by the Earth Resources Laboratory Founding Member Consortium and Air Force Laboratory Contract F19628-03-C-0126. Additional partial support came from the Shell Gamechanger Program.

REFERENCES

Aminzadeh, F., J. Brac, and T. Kunz, 1997, 3-D salt and overthrust models: SEG/EAGE.

Bakulin, A., and R. Calvert, 2004, Virtual source: new method for imaging and 4D below complex overburden: 74th Annual International Meeting, SEG, Expanded Abstracts, 2477–2480.

Calvert, R.W., A. Bakulin, and T. C. Jones, 2004, Virtual sources, a new way to remove overburden problems: 66th Annual International Meeting, EAGE, Extended Abstracts, 234.

Cassereau, D., and M. Fink, 1992, Time-reversal of ultrasonic fields-part III: theory of the closed time-reversal cavity: IEEE Transactions in Ultrasonics, Ferroelectrics and Frequency Control, **39**, 579–592.

de Hoop, M. V., and A. T. de Hoop, 2000, Wave-field reciprocity and optimization in remote sensing: Proceedings of the, Royal Society of London, Series A, Mathematical and Physical Sciences, **456**, 641–682.

Derode, A., E. Larose, M. Tanter, J. de Rosny, A. Tourin, M. Campillo, and M. Fink, 2003, Recovering the Green's function from field-field correlations in an open scattering medium (L): Journal of the Acoustical Society of America, **113**, 2973–2976.

Derode, A., A. Tourin, and M. Fink, 2000, Limits of time-reversal focusing through multiple scattering: long range correlation: Journal of the Acoustical Society of America, **107**, 2987–2998.

Draeger, C., D. Cassereau, and M. Fink, 1997, Theory of the time-reversal process in solids: Journal of the Acoustical Society of America, **102**, 1289–1295.

Fink, M., 1992, Time reversal of ultrasonic fields – Part I: basic principles: IEEE Transactions in Ultrasonics, Ferroelectrics and Frequency Control, **39**, 555–566.

Fink, M., and D. Cassereau, 2000, Time reversed acoustics: Reports on Progress in Physics, **63**, 1933–1994.

Fink, M., and J. de Rosny, 2002, Time-reversed acoustics in random media and chaotic cavities: Nonlinearity, **15**, R1–R18.

Jonsson, L., M. Gustafsson, V. Weston, and M. de Hoop, 2004, Retrofocusing of acoustic wavefields by iterated time reversal, SIAM Journal on Applied Mathematics, **64**, 1954–1986.

Malcolm, A., J. Scales, and B. van Tiggelen, 2004, Extracting the Green function from diffuse, equipartitioned waves: Physics Review E, **70**, 015601-1–015601-4.

Schuster, G., F. Followill, L. Katz, J. Yu, and Z. Liu, 2003, Autocorrelogram migration: theory: Geophysics **68**, 1685–1694.

Schuster, G., J. Yu, J. Sheng, and J. Rickett, 2004, Interferometric/daylight seismic imaging: Geophysical Journal International, **157**, 838–852.

Snieder, R., 2004, Extracting the Green's function from the correlation of coda waves: a derivation based on stationary phase: Physics Review E, **69**, 46610.

van Manen, D. J., J. Robertsson, and A. Curtis, 2005, Modeling of wave propagation in inhomogeneous media: Physical Review Letters, **94**.

Wapenaar, C. P. A., and J. T. Fokkema, 2005, Seismic interferometry, time-reversal and reciprocity: 67th Annual International Meeting EAGE, Extended Abstracts, G-031.

Wapenaar, K., 2004, Retrieving the elastodynamic Green's function of an arbitrary inhomogeneous medium by cross correlation: Physical Review Letters, **93**.